Article

Reaction of Au(PPh)Cl with Thiols Yields Thiolate Monolayer Protected Au Clusters

Ramjee Balasubramanian, Rui Guo, Allan J. Mills, and Royce W. Murray

J. Am. Chem. Soc., **2005**, 127 (22), 8126-8132• DOI: 10.1021/ja050793v • Publication Date (Web): 13 May 2005

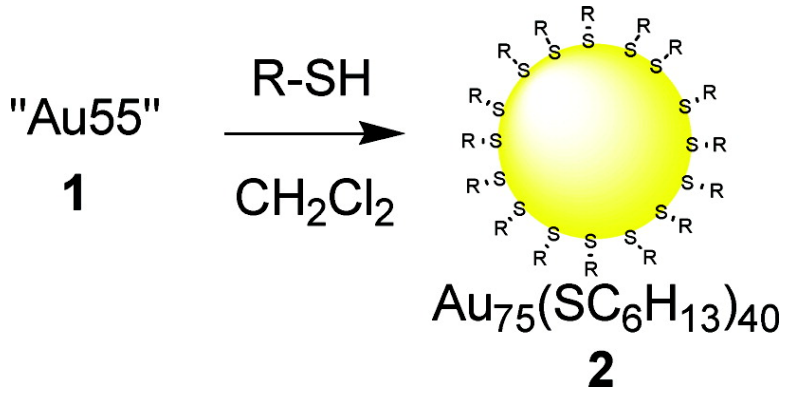

More About This Article

Additional resources and features associated with this article are available within the HTML version:

- Supporting Information
- Links to the 31 articles that cite this article, as of the time of this article download
- Access to high resolution figures
- Links to articles and content related to this article
- Copyright permission to reproduce figures and/or text from this article

View the Full Text HTML

J|A|C|S
ARTICLES
Published on Web 05/13/2005

Reaction of $Au_{55}(PPh_3)_{12}Cl_6$ with Thiols Yields Thiolate Monolayer Protected Au_{75} Clusters

Ramjee Balasubramanian, Rui Guo, Allan J. Mills,† and Royce W. Murray*

Contribution from the Kenan Laboratories of Chemistry, University of North Carolina at Chapel Hill, Chapel Hill, North Carolina 27599

Received February 7, 2005; E-mail: rwm@email.unc.edu

Abstract: This paper describes the reaction of the phosphine-protected Au nanoparticle $Au_{55}(PPh_3)_{12}Cl_6$ (**1**, "Au55") with hexanethiol (**2**) and other thiols. The voltammetry of the reaction product **2** displays a well-defined pattern of peaks qualitatively reminiscent of Au_{38} nanoparticles, but with quite different spacing (0.74 ± 0.01 V) between the potentials of initial oxidation and reduction steps (electrochemical gap). Correction of this "molecule-like" gap for charging energy indicates a HOMO−LUMO gap energy of about 0.47 V. Voltammetry of the products (**3** and **4**) of reaction of **1** with C_3H_7SH and PhC_2H_4SH, respectively, is similar. Laser desorption/ionization mass spectrometry (LDI-MS) shows that **2** contains a high proportion of a core mass in the 14−15 kDa range, which is proposed to be Au_{75}. UV−vis spectra of **2**−**4** are relatively featureless, similar to previous reports of thiolate-protected Au_{75} nanoparticles. HPLC analysis of **2** shows a Au_{75} content of ca. 73%; the electrochemical purity estimate is also high, about 55%. Combining the mass spectrometric result with thermogravimetric analysis of **2** leads to a preliminary formulation $Au_{75}(SC_6H_{13})_{40}$. This Au_{75} synthesis complements a previous Brust-type synthesis and is unusual in the apparent provocation in the reaction of an increase in core size.

Introduction

Research on metal and semiconductor nanoparticles[1] of dimensions exhibiting quantized behaviors ("quantum dots") has surged in recent years due to interest in the size- and shape-dependent tailoring of their physical and chemical properties and their potential in applications in catalysis, sensors, and molecular electronics.[2] Thiolate monolayer-protected Au clusters (Au MPCs)[3] have been of interest in this regard, since among the various Au nanoparticle-stabilizing agents, the efficacy of thiolates is well-established.[4] An important synthetic route to thiolate-protected Au MPCs is Brust's two-phase method;[5] phase transfer[6] and ligand exchange reactions[7] have also been widely investigated. These are "bottom-up" procedures in which the nanoparticles are prepared from elementary substances. Reactions that lead to monodisperse (all the same size) nanoparticles of some anticipated size and/or that reflect an intrinsic thermodynamic stability (closed shell) of that particular cluster are a general goal in nanoparticle science, which is particularly challenging in the small-size, quantum dot regime. While moderate regulation of the average cluster size is possible by tuning reaction conditions,[8] MPC syntheses typically yield a dispersity of core sizes. This has placed a premium on isolation of specific core sizes by postsynthetic transformation, by techniques such as fractional precipitation,[3a] chromatographic methods such as size exclusion chromatography (SEC)[9] and high-pressure liquid chromatography (HPLC),[10] and chemical etching.[11] Quantum dot thiolate-protected Au MPCs with nuclearity of 11,[12] 13,[13a] 18,[13b] 21,[13b] 25,[13b] 28,[13b−d] 32,[13b] 38,[14]

† Department of Chemistry, University of Liverpool, Liverpool, U.K., L69 3BX.

(1) (a) Schmid, G., Ed. *Clusters and Colloids*; VCH: Weinheim, Germany, 1994. (b) Klabunde, K. J., Ed. *Nanoscale Materials in Chemistry;* John Wiley & Sons: New York, 2001.
(2) (a) Alivisatos, A. P. *J. Phys. Chem*. **1996**, *100*, 13226. (b) Rao, C. N. R.; Kulkarni, G. U.; Thomas, P. J.; Edwards, P. P. *Chem. Eur. J.* **2002**, *8*, 28. (c) Kamat, P. V. *J. Phys. Chem. B* **2002**, *106*, 7729. (d) Thomas, K. G.; Kamat, P. V. *Acc. Chem. Res.* **2003**, *36*, 888. (e) Shenhar, R.; Rotello, V. M. *Acc. Chem. Res*. **2003**, *36*, 549. (f) Cushing, B. L.; Kolesnichenko, V. L.; O'Connor, C. J. *Chem. Rev*. **2004**, *104*, 3893. (g) Schlögl, R.; Hamid, S. B. A. *Angew. Chem., Int. Ed.* **2004**, *43*, 1628. (h) Murphy, C. J. *Anal. Chem.* **2002**, *74*, 520A. (j) Feldheim, D. L.; Keating, C. D. *Chem. Soc. Rev.* **1998**, *27*, 1.
(3) (a) Whetten, R. L.; Khoury, J. T.; Alvarez, M. M.; Murthy, S.; Vezmar, I.; Wang, Z. L.; Stephens, P. W.; Cleveland, C. L.; Luedtke, W. D.; Landman, U. *Adv. Mater.* **1996**, *8*, 428. (b) Templeton, A. C.; Wuelfing, W. P.; Murray, R. W. *Acc. Chem. Res.* **2000**, *33*, 27.
(4) Daniel, M.-C.; Astruc, D. *Chem. Rev.* **2004**, *104*, 293.
(5) Brust, M.; Walker, M.; Bethell. D.; Schiffrin, D. J.; Whyman, R. *J. Chem. Soc., Chem. Commun*. **1994**, 801.
(6) (a) Sarathy, K. V.; Kulkarni, G. U.; Rao, C. N. R. *Chem. Commun*. **1997**, 537. (b) Balasubramanian, R.; Kim, B.; Tripp, S. L.; Wang, X.; Lieberman, M.; Wei, A. *Langmuir* **2002**, *18*, 3676.
(7) Hostetler, M. J.; Green, S. J.; Stokes, J. J.; Murray, R. W. *J. Am. Chem. Soc.* **1996**, *118*, 4212.
(8) Hostetler, M. J.; Wingate, J. E.; Zhong, C.-J.; Harris, J. E.; Vachet, R. W.; Clark, M. R.; Londono, J. D.; Green, S. J.; Stokes, J. J.; Wignall, G. D.; Glish, G. L.; Porter, M. D.; Evans, N. D.; Murray, R. W. *Langmuir* **1998**, *14*, 17.
(9) (a) Wilcoxon, J. P.; Martin, J. E.; Provencio, P. *Langmuir* **2000**, *16*, 9912. (b) Wilcoxon, J. P.; Provencio, P. P. *J. Phys. Chem. B* **2003**, *107*, 12949. (c) Al-Somali, A. M.; Krueger, K. M.; Falkner, J. C.; Colvin, V. L. *Anal. Chem*. **2004**, *76*, 5903. (d) Wellsted, H.; Sitsen, E.; Caragheorgheopol, A.; Chechik, V. *Anal. Chem*. **2004**, *76*, 2010.
(10) (a) Jimenez, V. L.; Leopold, M. C.; Mazzitelli, C.; Jorgenson, J. W.; Murray, R. W. *Anal. Chem*. **2003**, *75*, 199. (b) Song, Y.; Jimenez, V.; McKinney, C.; Donkers, R.; Murray, R. W. *Anal. Chem.* **2003**, *75*, 5088. (c) Song, Y.; Heien, M. L.; Jimenez, V.; Wightman, R. M.; Murray, R. W. *Anal. Chem.* **2004**, *76*, 4911.
(11) (a) Schaaff, T. G.; Whetten, R. L. *J. Phys. Chem. B* **1999**, *103*, 9394. (b) Prasad, B. L. V.; Stoeva, S. I.; Sorensen, C. M.; Klabunde, K. J. *Chem. Mater*. **2003**, *15*, 935.
(12) Woehrle, G. H.; Warner, M. G.; Hutchison, J. E. *J. Phys. Chem. B* **2002**, *106*, 9979.

10.1021/ja050793v CCC: $30.25

39,[13b] 75,[15] 116,[15a] and 140[16] (in the <200 range) have been reported, albeit with varying ease and quality of preparation.

An alternative approach to monodisperse thiolate-protected Au MPCs starts with samples of (ideally) monodisperse Au nanoparticles protected by a different ligand, such as phosphines, as templates of that size nanoparticle. In the early 1980s, Schmid reported[17] synthesis of phosphine monolayer-stabilized 1.4 nm (core diameter) Au nanoparticles (by reducing $(Ph_3P)AuCl$ with B_2H_6) that, based on Mossbauer and ultracentrifugation studies, were formulated as $Au_{55}(PPh_3)_{12}Cl_6$—a two-shell close-packed cuboctahedron structure of Au_{13} surrounded by 42 atoms. $Au_{55}(PPh_3)_{12}Cl_6$ ("Au55" or **1**) has limited stability in solutions—the phosphine ligands dissociate readily[18]—but has been reported to exhibit resistance to oxidation compared to bulk Au or Au nanoparticles of a different size.[19] Other investigations[20] of Au55 have revealed that preparations of this material are commonly polydisperse (containing nanoparticles of other nuclearities than Au_{55}).[21] Notable is a report by Fackler and co-workers[22] giving definitive evidence based on ^{252}Cf-plasma desorption mass spectrometry, that (a) the purity of Au55 samples prepared by different groups differed significantly, (b) their composition could change with time, but, (c) in freshly prepared or purified samples, peaks could be attributed to substantial amounts of Au_{55} nanoparticles. One freshly prepared sample of Au55 contained a mixture of 9.5, 14, and 20 kDa clusters, corresponding to possible core nuclearities of 39, 58, and 77 atoms.[22] Other reports of phosphine stabilized gold clusters of core nuclearities 39 [23] and ~75 [24] can also be found in the literature. A simpler Brust-type protocol was used by Hutchison for the synthesis of a 1.5 nm diameter (average, by transmission electron microscopy, TEM) phosphine-stabilized gold nanoparticles, formulated as $Au_{101}(PPh_3)_{21}Cl_5$.[25]

Scheme 1. Reaction between $Au_{55}(PPh_3)_{12}Cl_6$ and Thiol R−SH

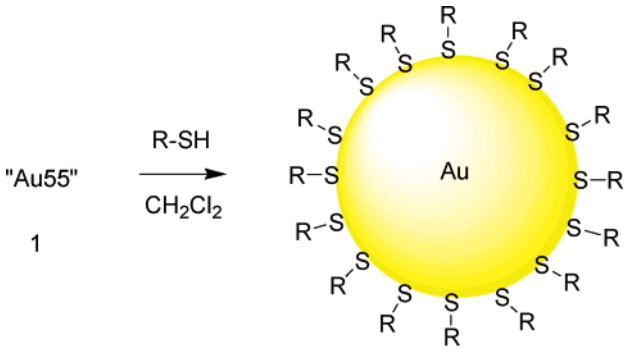

2. R = C_6H_{13}
3. R = C_3H_7
4. R = PhC_2H_4

The instability/polydispersity uncertainties not withstanding, Au55 continues to draw attention as an entry to the quantum dot metal nanoparticle regime,[26−29] including ligand replacements leading to other water-soluble phosphines.[26] Hutchison[27] and co-workers introduced the use of Au55 as a template to prepare both organic and aqueous soluble small thiolate-protected Au MPCs. In experiments reacting **1** with a variety of thiols as in Scheme 1, complete loss of phosphine and Cl ligands was established by X-ray photoelectron spectroscopy (XPS).[27] Similarly, Schmid reported the reaction of **1** with bulky thiols.[28] Hutchison[27] and Schmid[28] mainly relied on TEM for the core size determination, and there were notable differences in reported core sizes with the thiols employed. A detailed mechanistic study of the phosphine to thiolate replacement was recently reported.[29] Hutchison demonstrated that replacement of surface-bound phosphine in **1** by an amine incited a substantial increase in core size.[30] In contrast, the relatively well-studied thiolate-for-thiolate ligand replacements on Au MPCs lead to retention of the Au core size.[3b,7]

This paper describes reactions of thiols with **1**, namely, RSH = $C_6H_{13}SH$, C_3H_7SH, and PhC_2H_4SH in Scheme 1, with an aim analogous to that above, obtaining relatively monodisperse nanoparticles by reaction modification of a small-core size template species. In the study, following the previous mass spectrometric evidence[22] and other studies,[21b] we accept that use of synthetic protocols established by Schmid[17] produces polydisperse MPCs in which the Au_{55} core size is present in significant proportions. Using analytical approaches developed in previous MPC studies,[3,8] we establish that **1** is transformed not only in regard to its ligands, exchanging phosphine for thiolate, but also experiences a core size change to a larger core species, Au_{75}.

Experimental Section

Chemicals. Triphenylphosphine (Aldrich, 99%), ethanol (Aaper, 200 proof), sodium borohydride (Aldrich, 99%), boron trifluoride diethyl etherate (Aldrich), Celite (Aldrich, high purity analytical grade),

(13) (a) Negishi, Y.; Tsukuda, T. *J. Am. Chem. Soc.* **2003**, *125*, 4046. (b) Negishi, Y.; Takasugi, Y.; Sato, S.; Yao, H.; Kimura, K.; Tsukuda, T. *J. Am. Chem. Soc.* **2004**, *126*, 6518. (c) Schaaff, T. G.; Knight, G.; Shafigullin, M. N.; Borkman, R. F.; Whetten, R. L. *J. Phys. Chem. B* **1998**, *102*, 10643. (d) Link, S.; El-Sayed, M. A.; Schaaff, T. G.; Whetten, R. L. *Chem. Phys. Lett.* **2002**, *356*, 240.
(14) (a) Lee, D.; Donkers, R. L.; Wang, G.; Harper, A. S.; Murray, R. W. *J. Am. Chem. Soc.* **2004**, *126*, 6193. (b) Jimenez, V. L.; Georganopoulou, D. G.; White, R. J.; Harper, A. S.; Mills, A. J.; Lee, D.; Murray, R. W. *Langmuir* **2004**, *20*, 6864.
(15) (a) Alvarez, M. M.; Khoury, J. T.; Schaaff, T. G.; Shafigullin, M.; Vezmar, I.; Whettan, R. L. *Chem. Phys. Lett.* **1997**, *266*, 91. (b) Schaaff, T. G.; Shafigullin, M. N.; Khoury, J. T.; Vezmar, I.; Whetten, R. L.; Cullen, W. G.; First, P. N.; Gutierrez-Wing, C.; Ascensio, J.; Jose-Yacaman, M. J. *J. Phys. Chem. B* **1997**, *101*, 7885.
(16) Hicks, J. F.; Miles, D. T.; Murray, R. W. *J. Am. Chem. Soc.* **2002**, *124*, 13322.
(17) (a) Schmid, G.; Pfeil, F.; Boese, R.; Bandermann, F.; Meyer, S.; Calis, G. H. M.; van der Velden, J. W. A. *Chem. Ber.* **1981**, *114*, 3634. (b) Schmid, G. *Inorg. Synth.* **1990**, *27*, 214.
(18) Schmid, G. *Struct. Bonding* **1985**, *62*, 51.
(19) Boyen, H.-G.; Kästle, G.; Weigl, F.; Koslowski, B.; Dietrich, C.; Ziemann, P.; Spatz, J. P.; Riethmuller, S.; Hartmann, C.; Möller, M.; Schmid, G.; Garnier, M. G.; Oelhafen, P. *Science* **2002**, *297*, 1533.
(20) (a) Schmid, G. *Chem. Rev.* **1992**, *92*, 1709. (b) Schmid, G.; Corain, B. *Eur. J. Inorg. Chem.* **2003**, 3081.
(21) (a) Vogel, W.; Rosner, B.; Tesche, B. *J. Phys. Chem.* **1993**, *97*, 11611. (b) Rapoport, D. H.; Vogel, W.; Cölfen, H.; Schlögl, R. *J. Phys. Chem. B* **1997**, *101*, 4175. (c) Benfield, R. E.; Grandjean, D.; Kröll, M.; Pugin, R.; Sawitowski, T.; Schmid, G. *J. Phys. Chem. B* **2001**, *105*, 1961.
(22) (a) Fackler, J. P., Jr.; McNeal, C. J.; Winpenny, R. E. P.; Pignolet, L. H. *J. Am. Chem. Soc.* **1989**, *11*, 6434. (b) McNeal, C. J.; Winpenny, R. E. P.; Hughes, J. M.; Macfarlane, R. D.; Pignolet, L. H.; Nelson, L. T. J.; Gardner, T. G.; Irgens, L. H.; Vigh, G.; Fackler, J. P., Jr. *Inorg. Chem.* **1993**, *32*, 5582.
(23) Teo, B. K.; Shi, X.; Zhang, H. *J. Am. Chem. Soc.* **1992**, *114*, 2743.
(24) Gutiérrez, E.; Powell, R. D.; Furuya, F. R.; Hainfeld, J. F.; Schaaff, T. G.; Shafigullin, M. N.; Stephens, P. W.; Whetten, R. L. *Eur. Phys. J. D* **1999**, *9*, 647.
(25) Weare, W. W.; Reed, S. M.; Warner, M. G.; Hutchison, J. E. *J. Am. Chem. Soc.* **2000**, *122*, 12890.
(26) Schmid, G.; Klein, N.; Korste, L.; Kreibig, U.; Schönauer, D. *Polyhedron* **1988**, *7*, 605.
(27) (a) Brown, L. O.; Hutchison, J. E. *J. Am. Chem. Soc.* **1997**, *119*, 12384. (b) Warner, M. G.; Reed, S. M.; Hutchison, J. E. *Chem. Mater.* **2000**, *12*, 3316.
(28) (a) Schmid, G.; Pugin, R.; Malm, J.-O.; Bovin, J.-O. *Eur. J. Inorg. Chem.* **1998**, 813. (b) Schmid, G.; Pugin, R.; Meyer-Zaika, W.; Simon, U. *Eur. J. Inorg. Chem.* **1999**, 2051.
(29) Woehrle, G. H.; Brown, L. O.; Hutchison, J. E. *J. Am. Chem. Soc.* **2005**, *127*, 2172.
(30) Brown, L. O.; Hutchison, J. E. *J. Am. Chem. Soc.* **1999**, *121*, 882.

hexanethiol (Fluka, ≥95%), propanethiol (Aldrich, 99%), phenylethylthiol (Aldrich, 98%), acetonitrile (Fisher, ≥99.9%), and tetrabutylammonium perchlorate (abbreviated Bu_4NClO_4, Fluka, ≥99%) were used as received. Methylene chloride (Fisher, 99.9%), pentane (Fisher, 99.2%), benzene (Aldrich, 99+ %), and dimethoxyethane (Fluka, 99%) were dried and distilled according to standard procedures. $HAuCl_4$[31] was synthesized according to literature. Schmid's protocol was used for the synthesis of $Au_{55}(PPh_3)_{12}Cl_6$ (**1**).[17]

Au MPC Synthesis by Thiol Exchange. In a typical reaction, 10 mg of **1** dissolved in 5.5 mL of CH_2Cl_2 and 6 μL of $C_6H_{13}SH$ were stirred together at room temperature under Ar for 18 h. The reaction mixture was dried under reduced pressure and the residue dispersed in CH_3CN with mild sonication (~10 s), captured on a medium porosity glass frit, and washed copiously with CH_3CN (50 mL). Some (batch-dependent) loss of Au MPCs to the washings occurred in this step. The cleaned residue was removed from the frit by dissolution in CH_2Cl_2 to yield **2** (69 ± 18% yield based on mass, in five different synthetic batches).

Mass Spectrometry. A Micromass (TOFSPEC) instrument equipped with a 337 nm UV nitrogen laser (Laser Science Inc., Newton, MA) was used to obtain laser desorption−ionization time-of-flight (LDI-TOF) mass spectra in the positive ion mode. Details have been described previously.[14b]

Electrochemistry. Voltammetry was performed with a Bioanalytical Systems (BAS-100B) instrument on solutions containing (typically) 3 to 4 mg of the MPC product dissolved in 3 mL 0.1 M Bu_4NClO_4/CH_2Cl_2. Cyclic voltammetry (CV) and Osteryoung square-wave voltammetry (OSWV) were carried out in a single compartment cell containing 1.4 mm Pt disk working, Pt wire counter, and Ag wire quasi-reference (QRE) electrodes, under Ar. The working electrode was polished with 0.25 μm diamond paste (Buehler) and cleaned electrochemically by potential cycling in 0.5 M H_2SO_4. Low-temperature (233 K) voltammetry was carried out by immersing the cell in an acetonitrile/dry ice bath. The OSWV voltammograms were taken on freshly prepared solutions and were recorded with both positive- and negative-going potential scans, and values of peak potentials from the two scans were averaged to eliminate iR_{UNC} effects.

HPLC. HPLC experiments were done with an instrument equipped with a Waters 600 controller pump, a photodiode array detector (Waters 996 PDA), a Rheodyne 7725 injection valve with a 50 μL sample loop, and two serial stainless steel columns (silica bonded C8 250 × 4.6 mm i.d. stainless steel column, followed by a silica bonded phenyl 150 × 4.6 mm i.d. column, both with 5 μm particles; Thermo Electron Corp.). The mobile phase was 10 mM Bu_4NClO_4/CH_2Cl_2 at 0.7 mL/min. The MPC sample was filtered through a 0.45 μm Nalgene syringe filter with Teflon membrane prior to injection.

Other Measurements. Thermogravimetric analysis (TGA) was carried out in a Perkin-Elmer Pyris 1 thermogravimetric analyzer with 2−4 mg of MPCs in an Al pan at a heating rate of 10 °C/min. UV−vis data were obtained in a Shimadzu UV−visible spectrophotometer (UV-1601). ^{1}H NMR of Au MPCs in CD_2Cl_2 was recorded in a Bruker 400 MHz Avance spectrometer with a 5 s relaxation delay time.

Results and Discussion

Electrochemistry. The electrochemistry of quantum dot size Au MPCs exhibits two distinctive regimes of behavior: (a) MPCs of dimension Au_{140} and somewhat larger that display multiple one-electron core-charging peaks spaced roughly evenly on the potential axis at intervals explicable by "quantized double layer charging"[32−35] and roughly described by a concentric sphere capacitor model,[36] and (b) smaller core MPCs that display an enhanced spacing in the pattern of core-charging peaks, between the potentials for the first one-electron oxidation and for the first reduction. The enhanced spacing is interpreted[32] as reflecting the emergence of a "molecule-like" HOMO−LUMO band gap for the smaller core MPCs, of which $Au_{38}(SR)_{24}$ is a carefully investigated[14,35,37] example in the electrochemical sense. The electrochemical gap for $Au_{38}(SR)_{24}$ is 1.6 V, which[14] after correction for charging energy[38] to 1.3 eV agrees with the 1.3 eV obtained from optical band edge data, 1.3 eV.[39]

Reacting the nanoparticle Au55 with hexanethiol, a shorter alkyl chain thiol (C_3H_7SH), and an arene thiol (PhC_2H_4SH),[14a,40] in dichloromethane under Ar for ca. 18 h [27a] gave products labeled **2**−**4**, respectively. While the voltammetry of **1** exhibits no distinguishing peaks (possibly due to its polydispersity and consequent overlap of voltammetry of different components, as seen with thiolate-protected MPCs[41]), CV and OSWV of **2** do and are shown in Figure 1. These results clearly reveal a substantial electrochemical gap between the first oxidation peak (at ca. 0.22 V) and the first reduction (at ca. −0.51 V). The presence of the electrochemical gap (average 0.74 ± 0.01 V based on OSWV of five different synthetic batches) immediately reveals product **2** as a "molecule-like" species. An identical potential spacing (0.74 V) was seen before[32] for butanethiolate monolayer-protected clusters that had been characterized by mass spectrometry as having 14−15 kDa Au cores, consistent with the Au_{75} core formulation presented below.

The 0.74 ± 0.01 V electrochemical energy gap exceeds the actual HOMO−LUMO energy gap for **2** by the "charging energy". Charging energy reflects interactions between solvent and electrolyte and electrochemically charged nanoparticles. As done previously,[14a] we estimate charging energy from the 0.28 ± 0.01 and 0.25 ± 0.01 V potential differences between, respectively, the first and second oxidation steps and the first and second reduction steps (e.g., Figure 1b, see the asterisks (∗)). Deducting these values from the electrochemical gap gives an estimate for the actual HOMO−LUMO gap of 0.47 V. This energy gap is a little smaller than the previous ~0.6 eV estimate,[32] which was based on extrapolation of a low-energy optical band edge. The 0.47 eV result is smaller than that found (1.3 eV) for Au_{38}, as would be expected since **2** is, as shown below, a larger nanoparticle.[14,39]

The pattern of oxidation and reduction current peaks in the voltammetry of **2** in Figure 1 is reminiscent of the voltammetries[14] of $Au_{38}(SC_6H_{13})_{24}$ and $Au_{38}(SC_2H_4Ph)_{24}$, in that the first oxidation peak is promptly followed by a second peak, and then there is a slightly larger spacing 0.36 ± 0.02 V followed by

(31) *31. Handbook of Preparative Inorganic Chemistry*; Brauer, G., Ed.; Academic Press: New York, 1965; p 1054.
(32) Chen, S.; Ingram, R. S.; Hostetler, M. J.; Pietron, J. J.; Murray, R. W.; Schaaff, T. G.; Khoury, J. T.; Alvarez, M. M.; Whetten, R. L. *Science* **1998**, *280*, 2098.
(33) Hicks, J. F.; Templeton, A. C.; Chen, S.; Sheran, K. M.; Jasti, R.; Murray, R. W.; Debord, J.; Schaaff, T. G.; Whetten, R. L. *Anal. Chem.* **1999**, *71*, 3703.
(34) Miles, D. T.; Murray, R. W. *Anal. Chem.* **2003**, *75*, 1251.
(35) Quinn, B. M.; Liljeroth, P.; Ruiz, V.; Laaksonen, T.; Kontturi, K. *J. Am. Chem. Soc.* **2003**, *125*, 6644.
(36) Chen, S.; Murray, R. W.; Feldberg, S. W *J. Phys. Chem. B* **1998**, *102*, 9898.
(37) Yang, Y.; Chen, S. *Nano Lett.* **2003**, *3*, 75.
(38) (a) Franceschetti, A.; Zunger, A. *Phys. Rev. B* **2000**, *62*, 2614. (b) Creutz, C.; Brunschwig, B. S.; Sutin, N. *Compr. Coord. Chem. II* **2004**, *7*, 731.
(39) We have discussed previously[14a] the confusion between the energy gap data reported for $Au_{38}(SC_2H_4Ph)_{24}$ MPCs by us[14,32] and Quinn et al.[35] After that discussion, another nanoparticle, $Au_{38}(SC_6H_{13})_{24}$, has been described[14b] where the core mass was again supported by mass spectrometry and other analyses. The results in the new report[14b] support the assignment of a 1.3 eV HOMO−LUMO gap energy to the thiolate-protected Au_{38} core size.
(40) (a) Chen, S.; Murray, R. W. *Langmuir* **1999**, *15*, 682. (b) Wuelfing, W. P.; Murray, R. W. *J. Phys. Chem. B* **2002**, *106*, 3139.
(41) Miles, D. T.; Leopold, M. C.; Hicks, J. F.; Murray, R. W. *J. Electroanal. Chem.* **2003**, *554*−*555*, 87.

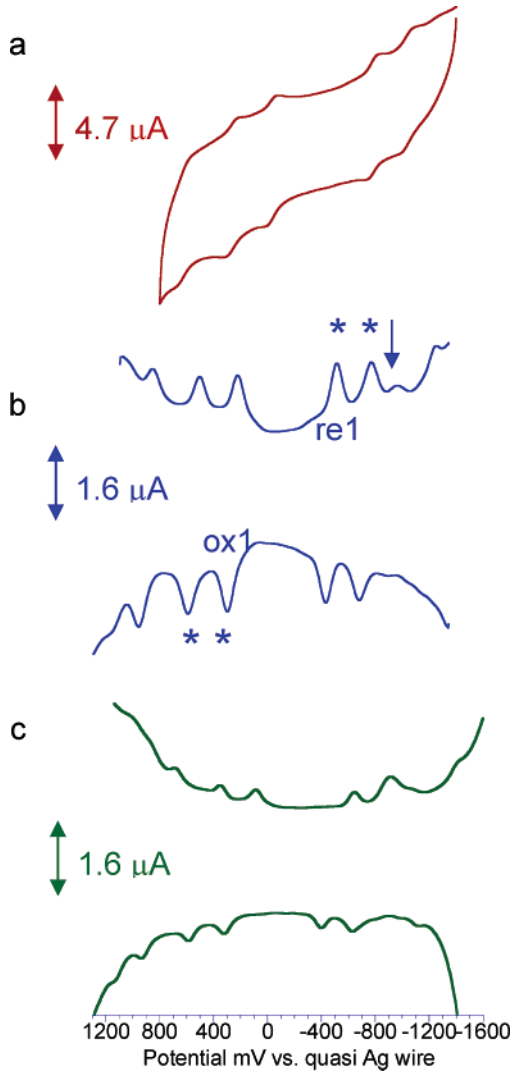

Figure 1. Voltammetry of 4 mg of the reaction product **2** between **1** ("Au55") and $C_6H_{13}SH$ in 3 mL of 0.1 M Bu_4NClO_4/CH_2Cl_2 under Ar atmosphere: (a) cyclic voltammetry at 284 K, potential scan rate 500 mV/s; (b) OSWV at 284 K (potential scan rate, 75 mV/s; pulse height, 5 mV; pulse cycle time, 66.7 ms); (c) OSWV at 233 K. Pt 1.4 mm diameter disk working electrode, Pt wire counter electrode, and Ag wire quasi reference electrode. The asterisks (∗) are peaks used to estimate charging energy (see text); the arrow indicates a spurious peak (see ref 42).

Scheme 2. Schematic Energy Level Diagram of **2** Based on Electrochemical Data Obtained in Dichloromethane[a]

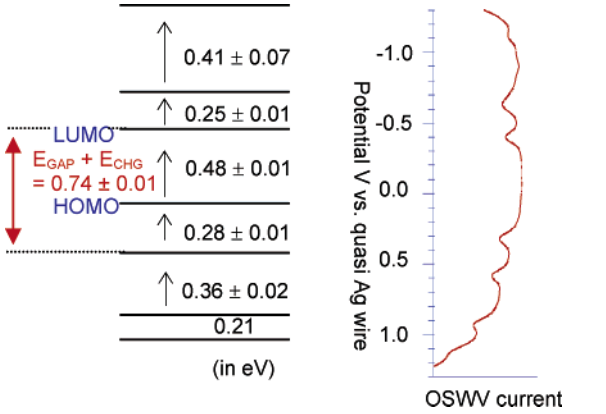

[a] A vertically aligned OSWV of **2** obtained at 233 K is provided at the right for reference.

another doublet of oxidation peaks (with spacing of ca. 0.21 V). The more positive current peaks are seen most clearly in a lowered temperature experiment (Figure 1c). As was the case for Au_{38}, multiply oxidized core states of **2** seem to be not very stable; the current peaks on the reverse (negative-going) potential scan are less distinct. The pattern of reduction peaks for **2** is on the other hand clearer than was the case for the Au_{38} MPCs, largely because they occur at less extremely negative potentials. Figure 1b shows that reduction proceeds as a doublet of steps spaced by 0.25 ± 0.01 V, with a 0.41 ± 0.07 V interval before another reduction step.[42] The first oxidation and reduction doublet of peaks are both cleanly seen in the cyclic voltammetry (Figure 1a).

As with the Au_{38} MPCs, we interpret the doublets of oxidation and reduction steps as successive losses of single electrons from doubly occupied molecular orbitals that lie, respectively, at the HOMO and LUMO energies of the molecule-like nanoparticle **2**. A third doubly occupied electronic orbital lies about 0.4 eV below the HOMO. These three well-defined electronic orbitals (two occupied and one above the Fermi level) are portrayed in Scheme 2 as a schematic of the electronic energy level structure of **2**. Scheme 2, which is qualitatively similar to that proposed[14a] for $Au_{38}(SC_2H_4Ph)_{24}$, was constructed mostly with data obtained in 284 K voltammetry studies with some inclusion of 233 K data. The numbers in Scheme 2 represent averages of voltammetry of five different preparations of **2**.

The voltammetry of products **3** and **4** from reaction of propanethiol and phenylethylthiol with Au55 is shown in Figure 2 (with that of **2** in Figure 2a, for comparison). The OSWV of **3** (Figure 2b) shows an electrochemical energy gap of 0.71 V, which upon correction for charging energy (0.25V from the oxidation doublet and 0.23 V from the reduction doublet) gives an estimated HOMO−LUMO gap of 0.47 V. The OSWV of **4** (Figure 2c) shows an electrochemical energy gap of 0.75 V; charging energy correction (0.27 V from oxidation doublet) gives an estimated HOMO−LUMO gap of 0.48 V. OSWV of **4** beyond the first reduction peak was almost featureless. While the results in Figure 2 are based on substantially less synthetic experimentation, they serve to show that the Au_{75} HOMO−LUMO gap is not highly sensitive to the thiolate ligand employed.

Mass and Electronic Spectra. Laser desorption/ionization−mass spectrometry (LDI-MS) and matrix assisted laser desorption/ionization−mass spectrometry (MALDI-MS) are powerful tools for characterization of Au clusters.[43] Significant recent results have also been obtained with electrospray ion sources.[13b,44] In LDI-MS, there is no efficient energy-dissipating matrix, and laser pulse volatilization of Au MPCs leads to the destruction

(42) Different batches of **2** sometimes displayed additional, lower magnitude current peaks; the peak in Figure 1b marked with an arrow is an example. Additional example voltammograms are found in Figure S-1. Presumably these features reflect sporadic presence of other core sizes. All of the potentials represented in Scheme 2 correspond to current peaks that were always present, as would have to be intrinsically so for a real substance. Additionally, after prolonged (>20 scans) cyclical potential scanning or at lowered temperature (233 K), the spurious additional peaks would sometimes appear, or currents for the "native" voltammetry became slightly enhanced. These phenomena are attributed, respectively, to decomposition effects or adsorption as seen before.[34] Spurious peaks can be significantly reduced by reacting the nanoparticle with additional hexanethiol in dichloromethane (for further details refer to Figure S-2).

(43) Schaaff, T. G. *Anal. Chem.* **2004**, *76*, 6187, and references therein.

(44) (a) Zhang, H.-F.; Stender, M.; Zhang, R.; Wang, C.; Li, J.; Wang, L.-S. *J. Phys. Chem. B* **2004**, *108*, 12259. (b) Zheng, J.; Petty, J. T.; Dickson, R. M. *J. Am. Chem. Soc.* **2003**, *125*, 7780.

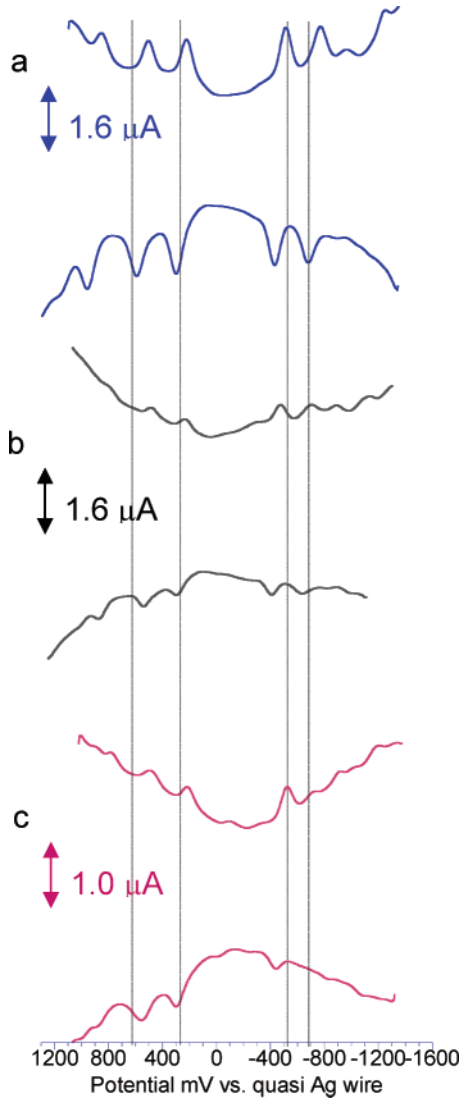

Figure 2. Osteryoung square-wave voltammetry of the products **3** (b) and **4** (c) of reaction between **1** ("Au55") and C_3H_7SH and $PhCH_2CH_2SH$, respectively, compared to that of **2** (a). Conditions are the same as Figure 1b. The formal potentials are aligned at ca. +0.3 V to facilitate comparison.

of the ligand monolayers, leaving only $[Au_N]^-$ or $[Au_NS_x]^-$ (or their positive counterparts) for mass analysis and detection. Both positive and negative ion modes can be used.[43]

Results for LDI-MS of the reaction product of **1** with hexanethiol, e.g., **2** in positive-ion mass spectral mode are shown in Figure 3. The "as prepared" sample of **2** gave a spectrum with mass centered at m/z = 14.5 kDa. The spectral fine structure (see inset) are ions separated by 200−220 Da, corresponding to losses of Au or Au−S moieties from the main fragment ion. Although the 14.5 kDa ions are the dominant species, it is evident that some ca. 10 kDa MPCs are present, as well as MPCs with masses around 22 and 29 kDa. Figure 3 shows no evidence for ~100 atom gold cores.[25] The evident polydispersity of the sample is consistent with the substantial level of background currents seen in the voltammetry of Figures 1 and 2. The presence of secondary peaks as a result of aggregation in the absence of a diluting matrix is also known in the literature.[3a] A very similar spectrum was obtained (data not shown) from a second sample of **2**, synthesized from a different batch of **1**.

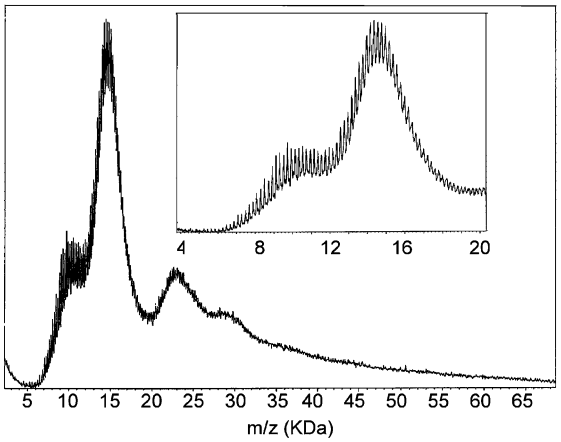

Figure 3. Laser desorption/ionization mass spectra (LDI-MS) of **2**. Inset: expanded scale for mass/charge from 4 to 20 kDa.

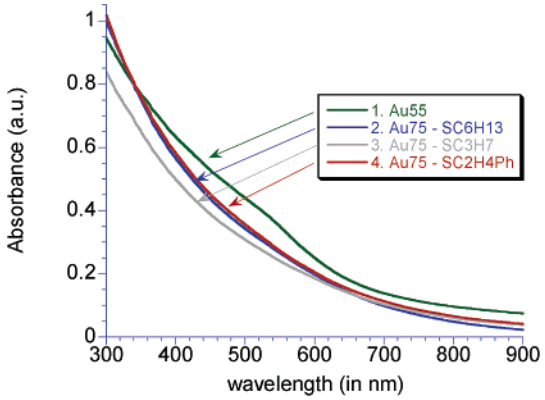

Figure 4. UV−vis spectra of **1**−**4** in CH_2Cl_2.

The isolation of Au clusters in the 14−15 kDa range protected with thiolate[11a,15a] and with phosphine[24] ligands has been previously established from mass spectral data. Those MPCs were prepared using the Brust synthesis[5] followed by purification steps. Except for the peaks at 22 and 29 kDa, Figure 3 is in fact quite similar to a spectrum of a reported 14 kDa nanoparticle (Figure 1a, ref 11a). This correspondence strongly indicates that we have prepared a Au_{75} thiolate-protected MPC by a different route, namely, through **1** as a precursor and small-size "template". That a core size change takes place in the thiolate-for-phosphine exchange is evident from Figure 3.

Optical absorbance spectra of size-separated Au clusters are well-documented in the literature.[45] For MPCs < 2 nm (core diameter), the surface plasmon resonance band (~520 nm) observed in larger Au colloids is absent, and the spectrum shows a more or less smoothly decreasing absorbance from the UV to low-energy visible region. For very small clusters such as Au_{38}, the presence of condensed energy level structures leads to fine structure atop the absorbance envelope (called "steplike").[14] We do not see such fine structure for samples of **2**−**4**, as shown by the spectra in Figure 4. Figure 4 also shows an example spectrum of **1**, which is similarly featureless except for a minor feature at ~520 nm, which has also been reported in parent Au55.[21b,27a] The featureless spectra of **2**−**4** are very similar to the earlier reports on Au_{75}.[11a] It is possible that the polydispersity of these materials washes out some intrinsic spectral details.

(45) Alvarez, M. M.; Khoury, J. T.; Schaaff, T. G.; Shafigullin, M. N.; Vezmar, I.; Whetten, R. L. *J. Phys. Chem. B* **1997**, *101*, 3706.

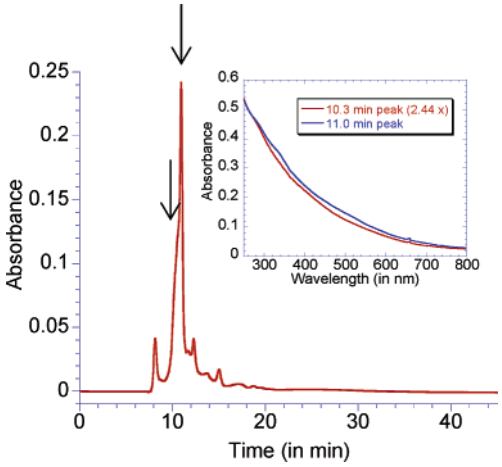

Figure 5. HPLC of **2** using serial columns (silica-bonded C8 column followed by a silica-bonded phenyl column) and 10 mM Bu_4NClO_4/CH_2Cl_2 as mobile phase, detected by PDA at 400 nm. Inset: UV−vis spectra obtained from PDA detector for the major peak (11 min) and its shoulder (10.3 min).

Separations. Chromatographic separations of metal nanoparticles have progressed rapidly in the past several years, with both gel permeation[9] and HPLC approaches.[10] Our HPLC studies have shown[10] that, on C8 columns, alkanethiolate-protected MPCs in the 1−2 nm core size range are resolved in a reverse-phase pattern in which smaller, more polar MPCs elute first followed by larger ones. Chemical functionality of the monolayer influences the separation pattern, and resolution was enhanced by use[14b] of serial columns of silica-bonded C8 and phenyl particles.

Figure 5 shows a typical HPLC separation of **2**, using serial columns. The major peak at ∼11 min is preceded by an unresolved shoulder at ∼10.3 min. PDA spectra of the two unresolved components are similar except that the 11 min component shows faint inflections at ca. 320 and 500 nm not evident in the other spectrum. PDA-based spectra of the other, minor chromatographic bands were noticeably different, reflecting polydispersity of the sample. The early-eluting minor peak's spectrum does not match the distinctive[14] fine structure of the Au_{38} MPC spectrum, so its presence in **2** can be ruled out. Co-injection of authentic $Au_{140}(SC_6H_{13})_{53}$ showed that the minor peak at ∼17 min is likely a Au_{140} MPC, consistent with the 29 KDa peak shown in Figure 3.

Thermogravimetric Analysis. Thiolate-protected MPCs are known to decompose thermally by liberation of the ligands as volatile disulfides,[8] leaving behind the (now aggregated) Au cores. TGA experiments thus give a convenient measure of the weight fraction of the MPC that is comprised in the organic thiolate monolayer. The thermal decomposition of the thiolate ligand monolayers of **2** (Figure 6) results in a mass loss of 23.9 ± 0.1% (samples from two different synthetic batches). Combining this result with the Figure 3 mass spectral evidence showing that the predominant core size in **2** is Au_{75} leads to a formulation of the composition of **2** as $Au_{75}(SC_6H_{13})_{40}$. The calculated ligand number assumes that the MPC cores of **2** are entirely Au_{75}, which given the dispersity is an approximation (see below). The $Au_{75}(SC_6H_{13})_{40}$ formulation should be considered as a preliminary one with respect to the thiolate ligand count.

Estimation of the Purity of 2. The purity of a Au MPC sample can be roughly estimated from chromatographic peaks

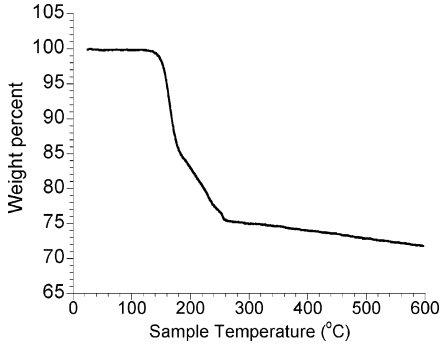

Figure 6. Thermogravimetric decomposition of **2**.

detected by optical absorbance, assuming a relatively constant absorbance coefficient per Au atom so that relative peak areas translate to relative masses of Au per peak. The integrated area of the major 11 min peak (with 10.3 min shoulder) in the Figure 5 chromatogram of the **2** peak area is 73 ± 9% (from 7 different synthetic batches) relative to the total chromatographic peak area. That is, the species responsible for the major peak represents about 73% of the Au mass in the sample of **2**.

MPC dispersity measured from voltammetry is based[16] on the relative sizes of the OSWV current peaks in **2** that are attributed to Au_{75} MPCs and the continuum background current envelope under the peaks (see Figure 1). The latter currents reflect a mixture of MPCs of varied sizes whose voltammetric peaks are not distinct due to overlap,[41] plus of course natural background currents from parasitic processes. The relative peak and continuum currents reflect relative concentrations of the species diffusing to the electrode. On this basis, the (presumed Au_{75}) peaks in Figure 1 comprise about 55 ± 3% of the total MPC concentration (from two batches, using peaks on either side of the electrochemical gap in Figure 1b). (In comparison, this purity criterion applied to Au_{140} MPCs has given monodispersity levels ranging from 20 to 80%.) The electrochemical result is probably an underestimate since the contribution from parasitic background currents is ignored.

The concentration percentage of the electrochemically distinctive species seen in the Figure 1 voltammetry of **2** is sufficiently high (55%) to support a presumption that the similarly dominant (73%, masswise) chromatographic peak in Figure 5 corresponds to the same species. The mass spectrometry in Figure 3 shows that the dominant species present in **2** has mass 14.5 kDa, which we assign to a Au_{75} core. It follows that the voltammetry and chromatography of Figures 1 and 5, respectively, also reflect the Au_{75} MPC and that its purity is between 55 and 73%.

TEM is commonly used to estimate the dispersity of core sizes of samples of nanoparticles. It tends to become less useful and reliable, however, with very small nanoparticles because of the difficulty[9a] of obtaining an adequate level of size resolution concurrently with a statistically representative collection of well-resolved images (meaning several 100's). Earlier studies[32] estimated the Au_{75} diameter by TEM as 1.35 nm, comparable to the 1.4 nm reported for Au_{55}.[21b] We could not

(46) Carbon coated copper grid or Formvar/carbon coated copper grid were used for the analysis. Solvents such as hexane, dichloromethane, toluene were used to dissolve the MPCs, and a drop of the sample was placed on the grid and left to dry. The TEM analyses were carried out in a Phillips CM12 side entry microscope operating at 100 keV. Scion image beta release and Image J software were used for data analysis.

obtain consistent TEM images of **2**. Despite the moderately good purity indicated by voltammetry and chromatography, TEM size estimates varied significantly.[46] In some examples, the TEM analysis gave estimates similar to those reported by Hutchison,[27a] but with a larger dispersion (data not shown).

Conclusion

The mass spectral data (on **2**) and electrochemical data (on **2**−**4**), coupled with the previous[11a,15a,32] evidences for Au_{75}, demonstrate that the major product of the reaction of **1** with hexanethiol is a thiolate-protected Au_{75}, with preliminary ligand composition $Au_{75}(SC_6H_{13})_{40}$. This synthesis of thiolate-protected Au_{75} augments the existing Brust-type synthesis/isolation developed by Whetten. It does so, curiously, starting with an MPC of a different core atom count, i.e., $Au_{55}(PPh_3)_{12}Cl_6$. A portion of the ligand reaction product may have a mass consistent with a Au_{55} moiety (Figure 3) but in yield much smaller than the evident Au_{75} product. The spurious peaks mentioned[42] in the electrochemistry in Figure 1 and the chromatography in Figure 5 both indicate that other species are present, but we are unable to make an assignment there to a Au_{55} component.

We are pushed to the hypotheses that either (a) the original **1** (made by the Schmid[17] protocol) contains a substantial portion of a Au_{75} phosphine-protected species (noting previous observations on the laboratory-dependent composition and homogeneity of **1**[22b]) that converts efficiently to thiolate-protected Au_{75}, while the Au_{55} component either does not or is unstable when thiolated, or (b) the source of Au_{75} MPCs in product **2** appears via a process(es) that causes an average increase in the original Au_{55} core size. The first hypothesis is quite weak,[47] given that that the mass yield of **2** synthesized from **1** can be as high as 93%, arguing against the possibility that the Au_{75} MPC is formed solely from a phosphine-protected Au_{75} in the **1** starting material. Considering the core-growth hypothesis, it is relevant to point to concurrent studies[48] in this laboratory in which a reverse reaction, of a $Au_{38}(SC_2H_4Ph)_{24}$ with triphenylphosphine, leads to a *loss* of Au from the nanoparticle core. The explanation may be speculated to lie in the large differences in the basicity of thiolate and phosphine ligands in the nonwater solvent and the relative stability of Au-carrying moieties such as Au^I-(thiolate) complexes.

Acknowledgment. This research was supported by grants from the National Science Foundation and Office of Naval Research. The authors thank Benjamin Pierce (Department of Chemistry, UNC) for help with the TGA measurement.

Supporting Information Available: Further examples of voltammetry and NMR spectrum (PDF). This material is available free of charge via the Internet at http://pubs.acs.org.

JA050793V

(47) It is notable that Fackler[22b] showed "Au_{55}" preparations subjected to a second celite column purification step always display a dominant mass spectral peak around 14 kDa. Our reaction of such additionally purified (celite with 10% pyridine/methylene chloride) "Au_{55}" with $C_6H_{13}SH$ gave CV and DPV responses similar to (but somewhat less well defined) those in Figure 1 and S-1, from materials not additionally purified.

(48) Wang, W.; Murray, R. W. Manuscript under preparation.